

Polyolefin blends

Part 3 *Morphology, thermal behaviour and mechanical properties of IPP-EPR alloys crystallized at low undercoolings*

R. GRECO, E. MARTUSCELLI, G. RAGOSTA

Istituto di Ricerche su Tecnologia dei Polimeri e Reologia del CNR, Arco Felice, Napoli, Italy

YIN JINGHUA

Changchun Institute of Applied Chemistry, Academia Sinica, Changchun, Jilin, China

Morphology observations, differential scanning calorimetry investigations and mechanical tensile tests have been performed on blends based on isotactic polypropylene and high-density polyethylene, containing ethylene-propylene (EP) copolymers of different composition. The blends after melting have been crystallized at low undercoolings ($T_c = 126$ and 110°C , respectively). All the properties strongly depend on the EP composition, indicating a marked interaction between the C_2 or C_3 sequences in the copolymers and the two matrices. These features are compared with those observed in previous work for the same blends crystallized at high undercoolings (quenched in water). Some relevant differences with respect to the crystallization procedures used and to the resulting structures in the blends are discussed.

1. Introduction

In previous papers [1, 2] we described the influence of ethylene-propylene copolymers (EPR), containing different ethylene (C_2) to propylene (C_3) ratios and various lengths of C_2 and C_3 sequences, on the morphology, structure, thermal behaviour, tensile and impact properties of blends between EPR and high-density polyethylene (HDPE) or isotactic polypropylene (iPP). Melt-mixing and compression-moulding followed by quenching in cold water was the procedure used in the preparation of the blend samples. It was found that a change in the C_2/C_3 ratio in the copolymers can induce variations in primary nucleating effects, in compatibility and in the perfection of crystallites. The mechanical tensile properties of initial unoriented specimens and fibres of both HDPE-EPR and iPP-EPR blends depend on the extent and the type of crystallinity of the EPR. The impact resistance of the blend, on the other hand, diminishes with respect to that of the parent homopolymers.

The present work is an extension of the previous study. The results of an investigation concerning the texture of spherulites, thermal behaviour and the stress-strain behaviour of specimens crystallized at low undercoolings of the same HDPE- and iPP-based blends are reported.

The main goal of this work is to examine the influence of the type and the extent of crystallinity of EPR on the morphology, structure and mechanical properties of HDPE-EPR and iPP-EPR blends crystallized at low values of undercooling, and to compare these results with those obtained in the case of samples crystallized non-isothermally at very high undercoolings.

2. Experimental procedure

2.1. Materials

The procedure of synthesis of ethylene-propylene (EP) copolymers has been reported in previous papers [1, 2]. The copolymer characterization is shown in Table I; this shows, from left to right, the code number (whose digits represent the molar percentage of propylene), the ratio of ethylene to propylene (C_2/C_3) in weight percentage, the intrinsic viscosity in decahydronaphthalene (135°C), the glass transition temperature, the index of crystallinity obtained at a given crystallization temperature ($T_c = 110$ and 126°C) and the melting points.

HDPE was supplied by the Rubber and Plastics Research Association of Great Britain (RAPRA) (Shrewsbury SY4 4NR), with $M_w = 1.1 \times 10^5$, $M_n = 1.1 \times 10^4$, MFI = 3.7. iPP (PPM 260) was produced by Exxon Chemical Co. with $M_w = 4.4 \times 10^5$, $M_n = 1.0 \times 10^5$.

2.2. Blend sample preparation

Blended materials (weight ratio iPP/EP = 80/20), obtained by melt-mixing in a Haake Rheocord equipment, were melted and pressed between two Teflon sheets in a hydraulic press at a temperature of 200°C and a pressure of about 240 atm. Then the pressure was released and the sandwiched samples were moved rapidly to a thermostated bath to be crystallized in about 14 h. For HDPE-based blends the crystallization temperature was 110°C and for iPP-based blends it was 126°C . The thickness of the sheets was 1 mm. Specimens were cut from these sheets and used for morphology observations, thermal behaviour investigations and determination of mechanical properties.

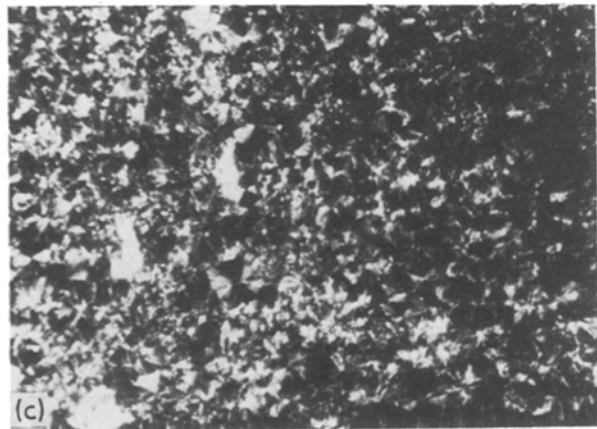
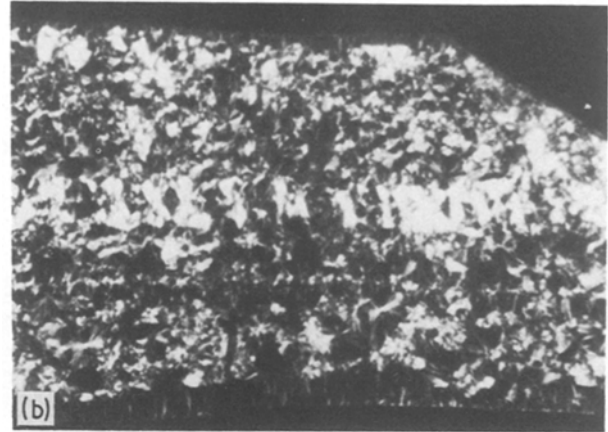
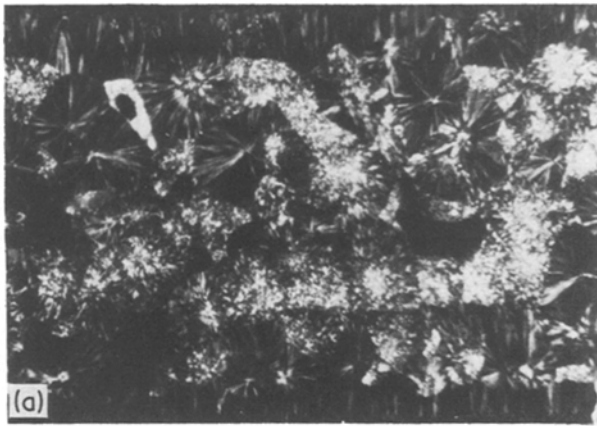


Figure 1 Transmission optical micrographs ($66\times$) of thin sections ($10\mu\text{m}$) of iPP and iPP-EP copolymer blends crystallized at 126°C for 14 h: (a) iPP, (b) iPP-EP88, (c) iPP-EP66.

2.3. Morphology

Thin sections to be observed by optical microscopy were obtained by using a Reichert-Sung microtome. Optical micrographs were taken by using a Wild Macroscope M420.

For the specimens observed by SEM, smooth surfaces were obtained by using the same microtome. Before the observation these surfaces were immersed in a $\text{CrO}_2\text{-H}_2\text{SO}_4$ saturated solution to etch out the amorphous phase from the smoothed surface. The method of preparation of the etching solution has been described in detail in previous papers [1, 2]. For iPP-based blends the etching temperature was 80°C and the etching time was 60 min, and for HDPE-based blends the temperature was 50°C and the time was

90 min. Finally the sections were coated with Au-Pd and observed by a Philips 501-13 SEM.

2.4 Thermal behaviour

The index of crystallinity X_c , melting temperature T_m and the width at half-height of the melting peaks of specimens were determined by using a Mettler TA 300 system apparatus. The rate of temperature increase was 10K min^{-1} . The weight of the specimens was about 5 mg. Values of $\Delta H^0 = 209$ and 290J g^{-1} were used for iPP and HDPE, respectively, to calculate the index of crystallinity.

2.5. Mechanical properties

The stress-strain behaviour of all the specimens was investigated by using an Instron testing machine, at room temperature and a crosshead speed of 10mm min^{-1} . Young's modulus E , yield strength σ_y and the constant stress at cold-drawing σ_c were calculated from the stress-strain curves.

3. Results and discussion

3.1. iPP-based blends

3.1.1. Morphology

Optical observations with crossed polars were made on thin sections of iPP homopolymer and blends made

TABLE I Composition, intrinsic viscosity, glass transition temperature, index of crystallinity and melting temperature of EPR

Code	C_2/C_3 (wt % ratio)	Intrinsic viscosity in decahydronaphthalene at 135°C (deg^{-1})	Glass transition temperature ($^\circ\text{C}$)	Index of crystallinity (%)*	Melting temperature ($^\circ\text{C}$)*
EP16	78/22	3.7	-50	27 ($T_c = 110^\circ\text{C}$) 27 ($T_c = 126^\circ\text{C}$)	124 [†] 124 [†]
EP31	60/40	2.4	-50	15 ($T_c = 110^\circ\text{C}$)	124 [†]
EP41	49/51	2.1	-44	13 ($T_c = 110^\circ\text{C}$)	124 [†]
EP55	35/65	1.7	-36	3 ($T_c = 110^\circ\text{C}$)	123 [†]
EP66	26/74	2.1	-33	9 ($T_c = 126^\circ\text{C}$)	148, 119, 80 [‡]
EP74	19/81	1.7	-20	15 ($T_c = 126^\circ\text{C}$)	148, 136, 100 [‡]
EP81	14/86	1.8	-10	28 ($T_c = 126^\circ\text{C}$)	148, 138, 115 [‡]
EP88	8/92	1.7	0 to 6	45 ($T_c = 110^\circ\text{C}$) 48 ($T_c = 126^\circ\text{C}$)	148 [†] 148, 139, 115 [‡]

* $T_c = 110, 126^\circ\text{C}$; crystallization time in 14 h.

[†] PE crystallinity.

[‡] PP crystallinity.

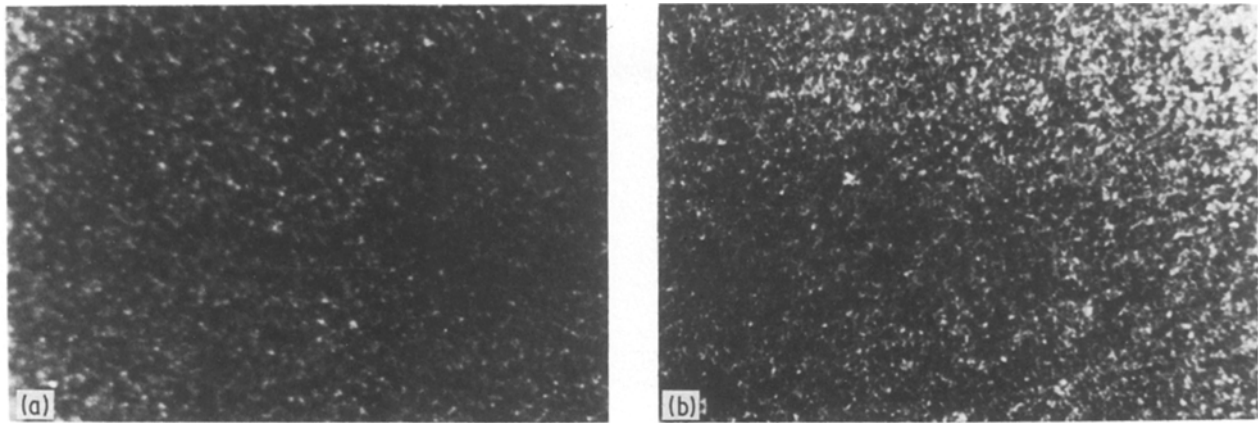


Figure 2 Transmission optical micrographs (59 ×) of thin sections (10 μm) of iPP-EP copolymer blends crystallized at 126°C for 14 h: (a) iPP-EP55, (b) iPP-EP16.

by iPP and all the EP copolymers (EP88, EP81, EP74, EP66, EP55, EP41, EP31 and EP16).

From such observations a striking feature comes out: for blends containing high C_3 -content copolymers (from EP88 down to EP66) there is only a small reduction of the iPP average spherulite size with respect to pure iPP, as shown in Figs 1a for iPP, 1b for iPP-EP88 and 1c for iPP-EP66 (the EP81 and EP74 microphotographs have been omitted). However, as soon as the C_3 content of the copolymers in the blend is further lowered to the EP55 value the texture becomes microspherulitic, and similarly for all the lower contents of C_3 . This is illustrated in Figs 2a for iPP-EP55 and 2b for iPP-EP16 blends (in this case the EP41 and EP31 microphotographs have been omitted).

This feature indicates a strong nucleating effect on iPP of the copolymers containing in their chains C_2 sequences (from EP55 to EP16). On the other hand, EP copolymers containing mainly C_3 crystallizable sequences (from EP88 to EP66) seem to have less influence on the iPP nucleation. The transition between the two modes lies in between the two copolymers EP66 and EP55, perhaps just in the vicinity of a C_2/C_3 ratio in moles of 60/40 or about 50/50 in weight.

It is worth pointing out at this point that the crystallization of iPP occurs at 126°C, where the low C_3 -content copolymers are still in a molten state (cf. Table I). Even though the phenomenon requires further investigation an attempt at explanation will be given here on the basis of the difference in mixability which can exist between the two copolymer series and the iPP. In fact the C_2 sequences of the copolymers EP55 to EP16 may easily segregate from the iPP in the melt before the slow iPP crystallization starts to occur. The preformed minidroplets can then act as heterogeneous nuclei for the iPP. When C_3 sequences are present in the copolymer chains in large amounts (EP88 to EP66) the compatibility with iPP in the melt is sufficiently high to limit segregation effects to very few anomalous chains (which can contain C_2 sequences). Therefore the nucleating effect is strongly reduced and a macrospherulitic texture is obtained, just as in the case of the iPP homopolymer. A decrease in the spherulite dimensions of iPP had been already described in literature for similar blends [3, 4]. It was

attributed to some poorly identified influence of the rubbers on the iPP crystallization.

The above hypothesis of iPP-EP miscibility at high C_3 content seems at a first sight to be in contrast with the results from small-angle neutron scattering recently presented by Lohse [5]. They show clear evidence, in fact, of a marked incompatibility in some iPP-EP blends with 50/50 weight ratio and containing very random EP copolymers of varying C_2/C_3 ratios. (The randomness can be only guessed at from the terms “amorphous” and “with some PP crystallinity” used by Lohse [5] in the characterization table). Our copolymers seem to be quite different, since they exhibit at high C_3 contents a considerable amount of crystallinity as well as high melting points (see Table I) and our blends have an iPP/EP weight ratio of 80/20. Therefore in our opinion the two sets of data are not necessarily in opposition. It is quite reasonable, in fact, that EP copolymers even at high C_3 content but with very short C_3 sequences are incompatible with iPP in a 50/50 blend, whereas they can be compatible if their block size is sufficiently high in an 80/20 alloy.

Electron micrographs of etched surfaces of iPP and of the blends containing high C_3 -content copolymers (EP88 to EP66) and EP16 (low C_3 ratio) are shown in Fig. 3. With a lowering of the C_3 content in the copolymers in the iPP-based alloys the following observations can be made:

- (i) The average spherulite size decreases slightly and gradually (no spherulite can be seen in Fig. 3f for the iPP-EP16 blend).
- (ii) The spherulites look less and less compact and perfect.
- (iii) More and more holes appear and the interspherulitic boundaries become wider and deeper.
- (iv) The iPP-EP16 micrograph shows a cheese-like appearance.

All these features are due to the strong oxidant action of the etchant on the amorphous regions, and this seems to confirm that the compatibility of the copolymers with the iPP matrix is a function of their C_3 content. In the case of iPP-EP16 the texture is microspherulitic and the EP16 is mostly rejected by the

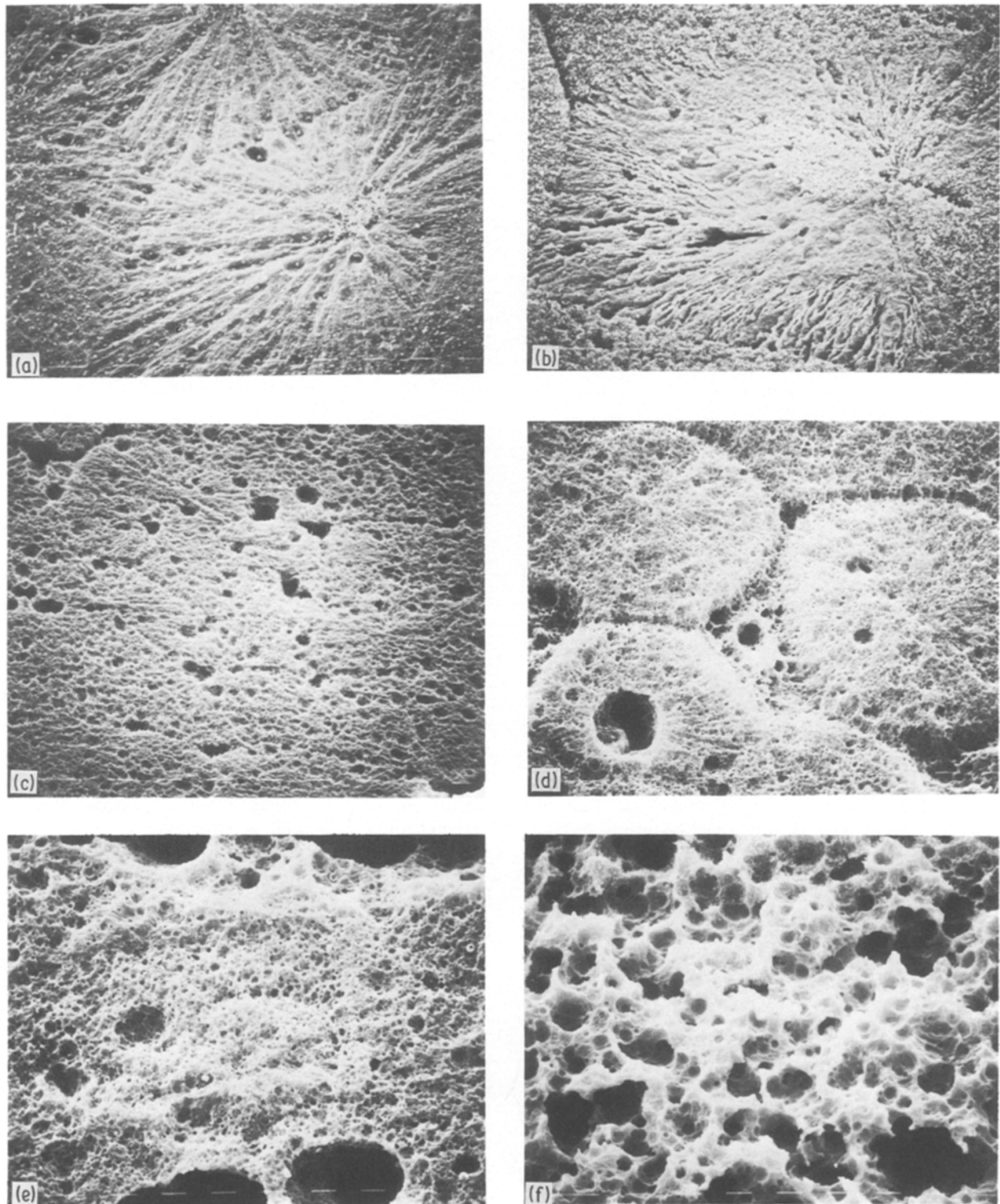


Figure 3 Scanning electron micrographs ($512\times$) of smoothed and etched surfaces of iPP and iPP-EP copolymer blends (for details see Section 2) crystallized at 126°C for 14 h: (a) iPP, (b) iPP-EP88, (c) iPP-EP81, (d) iPP-EP74, (e) iPP-EP66, (f) iPP-EP16.

growing iPP spherulite, creating domains well separated from the iPP. Therefore the treated surface shows numerous holes due to the extracted EP particles.

3.1.2. Thermal behaviour

The indices of crystallinity X_c and X_c^p , the melting temperature T_m and the width at half-height of the melting peak of isothermally crystallized pure iPP and iPP-EP copolymer blends ($T_c = 126^\circ\text{C}$) are shown in Table II. As indicated in previous papers [1, 2], X_c is the overall crystallinity experimentally obtained by differential scanning calorimetry (DSC), whereas X_c^p is

that calculated by the following equation (assuming no interaction between iPP matrix and EP copolymer domains):

$$X_c^p = W(\text{iPP})X_c(\text{iPP}) + W(\text{EP})X_c(\text{EP})$$

where $W(\text{iPP})$ and $W(\text{EP})$ are, respectively, the weight ratios of iPP and EP copolymers and $X_c(\text{iPP})$ and $X_c(\text{EP})$ are the crystallinities of pure iPP and EP copolymers crystallized at the same temperature (126°C) as the blends. The overall crystallinity X_c of every blends is decreased with respect to pure iPP. This is due to the fact that 20% of iPP is substituted

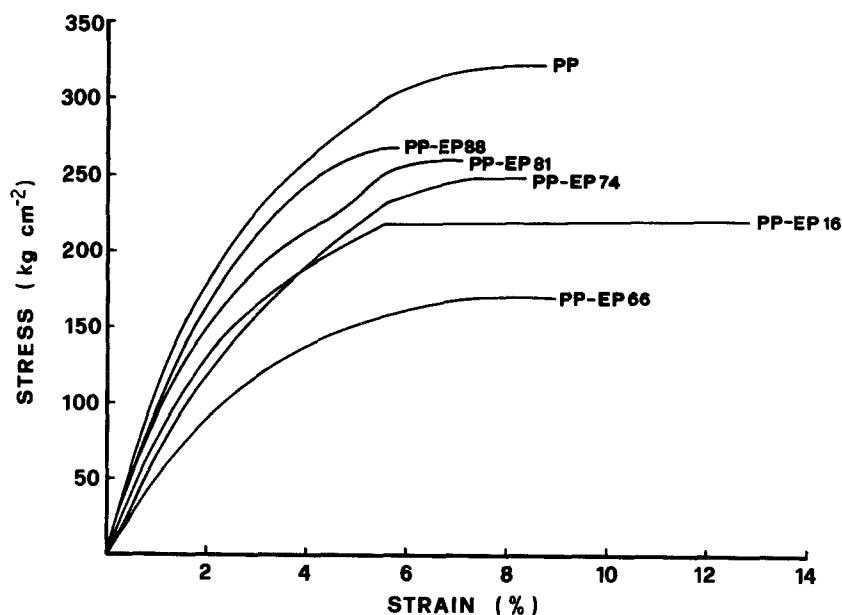


Figure 4 Stress-strain curves of iPP and iPP-EP copolymer blend specimens as indicated.

by a less crystalline copolymer. The extent of decrease depends, however, on the composition of the EP copolymer.

For all the blends the values of X_c and X_c^p coincide. The melting temperatures of all blends are lower than that of pure iPP. These features are completely different from those of the samples quenched in water. As shown in previous work [2] for the same blends, X_c^p was about 10 to 13% larger than X_c and the melting temperature was 6 to 10 K higher than that of pure iPP. For quenched samples these features were explained as follows: during the melt-mixing in the Brabender-like apparatus the EP copolymers might selectively extract and dissolve from the iPP matrix a certain amount of "defective" iPP molecules (having a higher than average concentration of steric defects and/or a lower molecular weight). This kind of segregation was probably still retained after the pressure release and the successive rapid crystallization. As the iPP matrix of the blends lost a certain amount of crystallizable defective molecules, X_c was lower than X_c^p and more perfect crystals were grown from the melt (a higher T_m appeared).

The different trend observed for samples crystallized at low undercoolings is accounted for by assuming that at high temperatures of crystallization the segregation of defective iPP molecules from the iPP matrix can be reversed to recover the original state. There is in fact a sufficient length of time (14 h) and a sufficiently high chain mobility at $T_c = 126^\circ\text{C}$ to

achieve this goal. The iPP matrix and the copolymer domains will separately crystallize and therefore almost no difference can be found between X_c and X_c^p [6]. As the copolymer crystals are less perfect than iPP [7] the melting temperatures of iPP-EP blends are slightly lower than that of pure iPP. Morphological effects should be also taken into account in order to explain such melting behaviour.

3.1.3. Mechanical properties

Typical stress-strain curves for pure iPP and iPP-EP blends crystallized at $T_c = 126^\circ\text{C}$ are shown in Fig. 4. All the specimens exhibit a brittle behaviour and rupture occurs before the neck formation. In contrast with this feature, specimens having the same composition but crystallized by quenching have a ductile behaviour, as shown in a previous paper [2]. The two opposite behaviours come from the different structures formed at high and low undercoolings, and especially depend on the nature of the amorphous materials bridging the crystallites. Some of the authors of this paper have explained in previous work [8, 9] similar features by the following considerations. For quenched specimens the crystallization occurs very rapidly and the chains retain almost completely the original entanglement network existing in the melt. Therefore the system is very interconnected all over the specimens by many tie-molecules (linking crystallites together). These tie-chains can effectively act as local load transducers and will yield therefore a ductile

TABLE II Index of crystallinity X_c , X_c^p , melting temperature T_m and width half-height of melting peaks for iPP-EP copolymer blends ($T_c = 126^\circ\text{C}$, crystallization time = 14 h) measured by DSC

Sample code	Index of crystallinity (%)		Melting temperature, T_m ($^\circ\text{C}$)	Width at half-height of melting peaks (K)
	X_c	X_c^p		
iPP	64	64	166	18
iPP-EP88	60	61	163	18
iPP-EP81	58	57	163	17
iPP-EP74	55	54	163	18
iPP-EP66	53	53	163	17
iPP-EP16	59	60	164	18

TABLE III Young's modulus E , tensile strength σ_b and elongation at break ϵ_b of iPP and iPP-EPR blends crystallized at low undercooling ($T_c = 126^\circ\text{C}$)

Sample code	$E(\text{kg cm}^{-2})$ $\times 10^{-4}$	$\sigma_b(\text{kg cm}^{-2})$ $\times 10^{-2}$	$\epsilon_b(\%)$
iPP	1.1	3.2	10
iPP-EP88	1.0	2.9	6
iPP-EP81	0.8	2.7	7
iPP-EP74	0.7	2.5	8
iPP-EP66	0.5	2.0	10
iPP-EP16	0.7	2.2	15

mechanical behaviour. In contrast, for specimens crystallized at high T_c , since the crystallization time is very long, most of the very mobile macromolecules are able to disentangle from each other. Hence only a few tie-molecules are left to bridge the crystallites. Furthermore these latter are very thick due to the long annealing time at $T_c = 126^\circ\text{C}$. Therefore, when an external force is applied, the spare tie-chains are unable to carry the load and to fracture the crystallites bridged by them. Therefore a brittle behaviour is the net result. The above explanations can be applied to the present system as well.

Another interesting feature can be seen from Fig. 4. The shape of stress-strain curves depends on the chemical composition, the extent and the type of crystallinity of EPR. This means that at the same strain the larger the C_3 content, the higher is the stress. The Young's moduli E calculated from the initial slope of the stress-strain curves, the tensile strength σ_b and the elongation at break ϵ_b of pure iPP and iPP-EPR blends are reported in Table III. The larger the crystallinity of the copolymer, the higher the values of E and σ_b for the related blend. These features can be attributed to the following facts: the higher the C_3 content in the copolymer, the better its compatibility with the iPP matrix (as mentioned earlier). The value of E for the iPP-EP16 blend is higher than those of the iPP-EP66 and iPP-EP74 blends. This is due to the larger crystallinity of EP16 copolymer. Another interesting feature is the higher elongation at break of such a blend with respect to all the other blends and to the same iPP homopolymer. This can be due to the different microspherulitic texture observed in Fig. 2b which can give, with respect to the interconnection of the system, an analogous effect to that of a slightly higher crystallization rate. Therefore even though the EP particles tend to hinder the cold drawing, the higher elongation value observed is attributable to the greater iPP matrix ductility.

3.1.4. General comparison with quenched blends

In the first paper of this series [1], iPP-EPR blends obtained by quenching in water exhibited (i) higher melting points and narrower melting peaks than pure iPP and (ii) a microspherulitic texture and ductile mechanical behaviour. The first effect was attributed to the extraction of defective iPP molecules by the EPR during the mixing with a consequently better perfection of the crystallites in the iPP matrix. The second effect is due to the high rate of cooling which yields a high density of heterogeneous nuclei and leaves an underlying structure of tie-molecules among the thin crystallites very close to the entanglement network, originally existing in the melt. Therefore the high interconnection throughout the system yields a very ductile behaviour.

The results illustrated in the present work for blends crystallized at low undercoolings (at a high crystallization temperature of 126°C) are the following: (i) no difference in melting points and half-width of the melting peaks; (ii) a macrospherulitic structure like that of pure iPP for C_3 copolymer contents larger than 0.66; (iii) a microspherulitic texture for C_3 contents less than 0.55; (iv) a brittle mechanical behaviour in all cases. The most striking feature is that similar microspherulitic textures show in one case (blends obtained at low T_c) a ductile behaviour and in another one (blends with copolymers at low C_3 content crystallized at high T_c) a brittle one. This indicates that no trust can be placed in the apparent morphology alone. The explanation lies in the diverse procedures that have been used to crystallize the blends. In the first case the texture is produced by a rapid cooling which activates a high density of nuclei; in the second one the same effect is achieved mainly by a heterogeneous nucleation due to the segregated C_2 sequences. What results as a real difference is the underlying network of tie-molecules and the different lamellar thicknesses produced by the diverse rate of cooling used in the two cases.

3.2. HDPE-based blends

3.2.1. Morphology

Optical observations reveal a microspherulitic structure for the HDPE homopolymer, for all the blends containing high C_2 -content copolymers HDPE-EP55, HDPE-EP41, HDPE-EP31 and HDPE-EP16, and also for the HDPE-EP88 copolymer with low C_2 content. Therefore no optical micrographs are reported in this paper.

TABLE IV Index of crystallinity X_c , X_c^p , melting temperature T_m and width at half-height of melting peaks for HDPE and HDPE-EP copolymer blends ($T_c = 110^\circ\text{C}$, crystallization time = 14 h) measured by DSC

Sample code	Index of crystallinity (%)		Melting temperature, T_m ($^\circ\text{C}$)	Width at half-height of melting peaks (K)
	X_c	X_c^p		
HDPE	88	88	140	16
HDPE-EP16	79	76	137	15
HDPE-EP31	76	73	137	15
HDPE-EP41	73	73	137	15
HDPE-EP55	73	71	137	15
HDPE-EP88	83	80	140	16

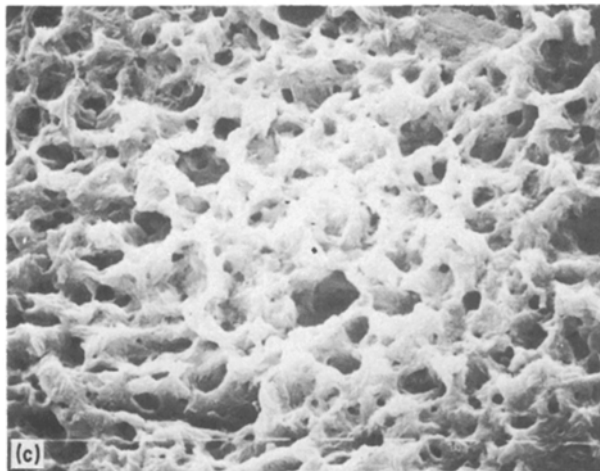
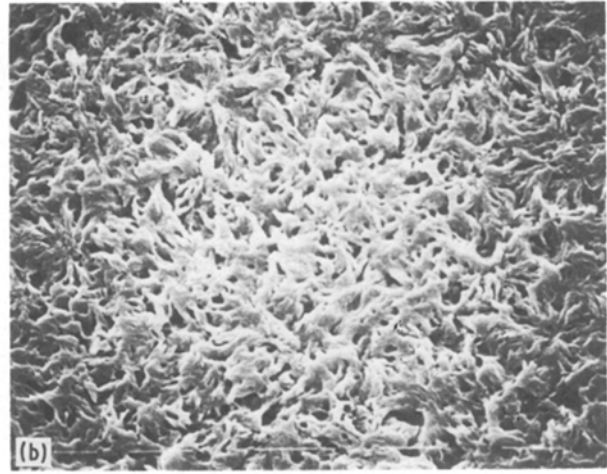
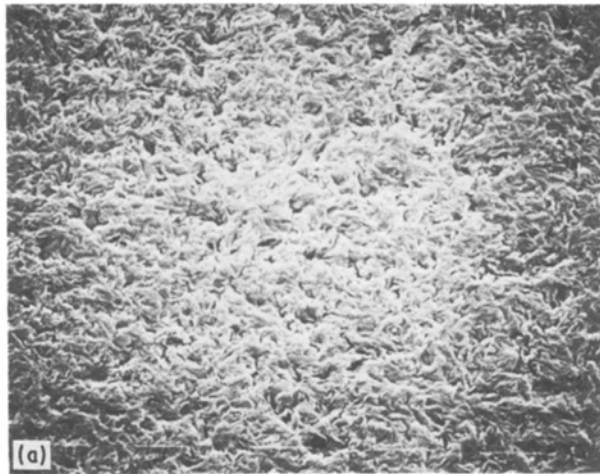


Figure 5 Scanning electron micrographs ($1118\times$) of smoothed and etched surfaces of HDPE and HDPE-EP copolymer blends crystallized at 110°C for 14 h: (a) HDPE, (b) HDPE-EP41, (c) HDPE-EP88.

Electron micrographs of etched surfaces are shown in Fig. 5 (5a for HDPE, 5b for HDPE-EP-41 and 5c for HDPE-EP88). As may be noted, the holes increase in number and size passing from pure HDPE to HDPE-EP41 (the behaviour of the various EPs with high C_2 content is very similar). A marked difference is obtained if the copolymer has instead a high C_3 content (EP88). In this case the texture is cheese-like as for iPP-EP16, indicating an easy extraction from the matrix of segregated EP particles. As for iPP-EP

blends, one could infer that the compatibility in the melt is going to decrease with decreasing C_2 content in the blend copolymer. However, in such a system the texture is already microspherulitic even in HDPE, and therefore no nucleating effect can be observed. This is due to the fact that homogeneous HDPE nucleation is already so efficient that the influence of heterogeneous nuclei becomes quite minor.

3.2.2. Thermal behaviour

For HDPE and HDPE-EP copolymer blends crystallized at low undercoolings the parameters of thermal behaviour obtained from the differential scanning thermograms are reported in Table IV. Similar features with those of pure iPP and iPP-EP copolymer blends appear and similar explanations can be offered for this type of blend.

3.2.3. Mechanical properties

Representative stress-strain curves of pure HDPE and HDPE/EPR blends are shown in Fig. 6. In contrast

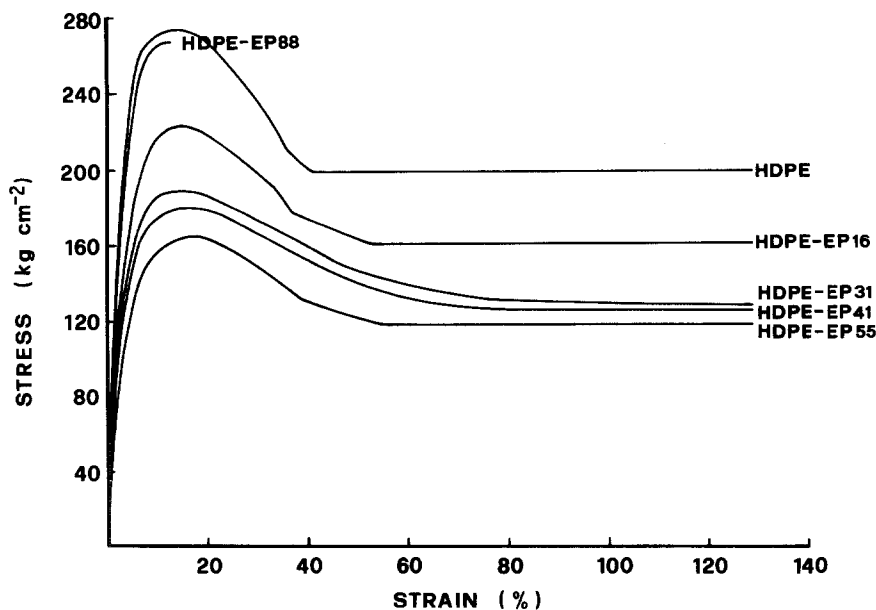


Figure 6 Stress-strain curves of HDPE and HDPE-EP copolymer blends as indicated.

TABLE V Young's modulus E , tensile yielding stress σ_y and the constant stress at cold drawing σ_c of HDPE and HDPE-EPR blends crystallized at low undercooling ($T_c = 110^\circ\text{C}$)

Sample code	$E(\text{kg cm}^{-2})$ $\times 10^{-3}$	$\sigma_y(\text{kg cm}^{-2})$ $\times 10^{-2}$	$\sigma_c(\text{kg cm}^{-2})$ $\times 10^{-2}$
HDPE	8.5	2.9	2.0
HDPE-EP16	6.2	2.2	1.6
HDPE-EP31	5.4	1.8	1.3
HDPE-EP41	5.0	1.8	1.3
HDPE-EP55	4.2	1.7	1.2
HDPE-EP88	8.9	2.7	-

with iPP-based blends all the specimens but one have a ductile behaviour. This can be attributed to the low glass transition temperature of the HDPE matrix and to the high nucleation rate of HDPE (yielding a micro-spherulitic structure).

For the HDPE-EP88 blend it must be taken into account that the EP88 copolymer is characterized by a high content of iPP crystallinity (48%, as shown in Table I) and the blend as a whole shows an X_c comparable to that of HDPE (see Table IV). Therefore the compatibility between the HDPE matrix and the EP88 copolymer domains is very poor and large EP88 domains are formed as confirmed by the morphology of its blend (Fig. 5). The final result is a high modulus (reinforcing effect) followed by a premature rupture since no cold drawing is allowed by the presence of the EP particles. As with the iPP-based blends, the slopes of curves and the values of the yield stress of blended systems depend on the content of C_2 sequences in the blends.

Young's moduli E , tensile yield stress σ_y and the constant stress at cold drawing σ_c (obtained from the stress-strain curves of the blends) are reported in Table V.

All these values are dependent upon the composition of the copolymer. It means that they increase with increasing C_2 content of the copolymer. These facts also can be tentatively attributed to the better compatibility and the higher crystallinity (Table III) of the blending system when the copolymer contains larger C_2 sequences. For the HDPE-EP 88 blend its larger values of E and σ_y with respect to all other blends come from its higher crystallinity content.

3.2.4. General comparison with quenched blends

The behaviours of blends crystallized at low and high undercooling are quite similar in the case of HDPE-EP alloys, since the crystallization rate of HDPE is so high that no real quenching is possible in the conditions used in the present paper. Therefore the morphology is micro-spherulitic and the mechanical behaviour ductile in both cases.

The only difference that still remains is in the thermal properties, compared with those of iPP-EP copolymer blends. In fact higher melting points and narrower melting peaks than those of pure HDPE are

shown by alloys crystallized at high undercooling. In the other case at $T_c = 110^\circ\text{C}$, lower T_m values for blends and equal half-widths of melting peaks with respect to pure HDPE are observed. This effect has already been explained for iPP-EP blends in a previous paragraph.

4. Concluding remarks

The results of the present paper relative to iPP-EP and HDPE-EP alloys crystallized at low undercoolings (high T_c s) in comparison with the same blends obtained at high undercoolings can be summarized as follows:

1. The morphology depends for iPP-EP blends both on the crystallization conditions as well as on the composition of the copolymer used. The mechanical properties, however, depend sharply on the former (all the systems show a brittle behaviour), and slightly on the latter.

2. In the case of HDPE-PE alloys the morphology and the mechanical properties show only a limited dependence on the crystallization conditions and on the copolymer composition (in all cases the mechanical behaviour is of a ductile nature but the parameters E , σ_y and σ_c depend markedly on the EP composition).

3. With respect to the thermal properties both iPP-EP and HDPE-EP alloys are analogously influenced by the crystallization conditions in terms of crystallinity, melting points and melting peak half-widths as well as by the copolymer C_2/C_3 ratios.

The hypothesis that at high C_3 (or C_2) content the copolymers are compatible somewhat with iPP (or HDPE) seems to rely on their block size, in contrast with some results obtained [5] on more amorphous copolymers of different blend composition.

Acknowledgements

The authors wish to thank Mr C. Mancarella for help in carrying out the experimental work.

References

1. R. GRECO, C. MANCARELLA, E. MARTUSCELLI, G. RAGOSTA and YIN JINGHUA, *Polymer* **28** (1987) 1922.
2. *Idem, ibid.* **28** (1987) 1929.
3. E. MARTUSCELLI, C. SILVESTRE and G. ABATE, *ibid.* **23** (1982) 229.
4. J. KARGER-KOCSIS, A. KALLÓ, A. SZAFNER, G. BODOR and Zs. SENYEI, *ibid.* **20** (1979) 37.
5. D. J. LOHSE, *Polym. Eng. Sci.* **26** (1986) 1500.
6. Z. BARTCZAK, A. GALESKI and E. MARTUSCELLI, *ibid.* **24** (1984) 1155.
7. R. GRECO, C. MANCARELLA, E. MARTUSCELLI, G. RAGOSTA and YIN JINGHUA, *Macromol. Chem.* **188** (1987) 2231.
8. R. GRECO and F. COPPOLA, *Plast. Rubb. Process Appl.* **6** (1986) 35.
9. F. COPPOLA, R. GRECO, E. MARTUSCELLI, H. W. KAMMER and C. KUMMERLOWE, *Polymer* **28** (1987) 47.

Received 29 October 1987

and accepted 25 February 1988